Journal of Harbin Engineering University
ISSN: 1006-7043

Vol 47 No. 07
July 2026

Torque Ripple Minimization in Switched Reluctance Motor Drives Using Torque Sharing Functions and Hybrid Meta-Heuristic Optimized Fractional Order Control for EV applications.

Adapa V C Janaki Ramayya[1], Venkata Reddy Kota[2]

[1]Research Scholar, Department of Electrical and Electronics Engineering, JNTUK, Kakinada-533003, AP, India.

[2]Professor & Head of the Dept, Department of Electrical and Electronics Engineering, JNTUK, Kakinada-533003, AP, India

Abstract

Switched Reluctance Motor (SRM) technology has gained significant attention in various industries due to its reliability, cost-effectiveness and efficiency. However, torque ripple remains a major issue, impacting the performance of SRM drives. To overcome this limitation, a proposed cascaded fractional-order controller is introduced to reduce torque ripple in SRM drives. The work begins with modelling the 8/6 SRM and analyzing its magnetic characteristics using MATLAB/Simulink. Then, the Torque Sharing Function (TSF) is applied to the SRM to generate the reference phase torque. These TSF-based torque profiles are then converted into reference phase currents using flux and current characteristics. In additional, cascaded fractional order proportional integral tilt and fractional order proportional integral with one plus proportional integral derivative filter (FOPIT-FOPI-(1+PIDN)) controller is proposed to improve speed and current regulation. An advanced optimization techniques, hybrid salamander orangutan optimization algorithm (HSOA), is used to fine-tune gain parameters and commutation angles. The result demonstrates significant improvements in torque ripple reduction of 0.45%, output power by 3346.07W, average torque of 6.8205 Nm and efficiency of 97.14%. These findings highlight the effectiveness of the proposed (FOPIT-FOPI-(1+ PIDN)) strategy in reducing torque ripple and improving efficiency, providing a promising solution for SRM-based drive systems.

Keywords: Torque ripples reduction, Switched reluctance motor, motor speed control, salamander optimization, and fractional order controller

1. Introduction

In several industrial applications, SRMs have generated significant interest. However, because of its resilience, easy fabrications and appropriate variable speed [1]. SRMs not requires permanent magnet, thus it is inexpensive for manufacturing [2]. The SRM motors have a few advantages, such as high-speed operations, lower energy losses and better winding dependability [3]. The boost converter in the SRM improves the power factor and the power supply. The switching strategies of the SRM will effectively optimize the efficiency [4]. Various control system is proposed to improve the performance of the SRMs, which include current chopping control (CCC), angle position control (APC), direct torquecontrol and model predictive control [5]. To avoid short-circuits across DC sources, the asymmetric bridge source drives the SRMs. The most challenging and important aspect of the SRM motor is torque ripple minimization [6]. The control strategies of SRM have both advantages and limitations, which suppress the torque ripple and also optimize the excitation parameters. But this strategy requires additional torque regulators for reducing torque values [7]. The modern industries with high speed application have increased the use of SRM, also used in the development of environmentally sustainable systems [8]. Recent review works have mentioned that SRM faced speed-related challenges, which affect the proper current control of the SRM [8]. The most common method for inherent torque ripple is Torque sharing functions (TSFs), here the reference torque is split between simultaneously providing torque from multiple phases using a determined profile such as cubic, linear, sinusoidal and partial functions [9]. Several approaches have been developed to improve the TSF, which include an optimization algorithm for enhancing the efficiency, reducing torque ripple and maximizing the torque per ampere ratio [10].

The switching angles of the SRM are optimized by the dung-beetle optimized back propagation (BP) neural network (DBO-BP) algorithm. To enable precision torque tracking flux theoretical derivation is adjusted dynamically [11]. The research mainly focuses on optimizing the control parameters such as current levels, supply voltage and turn-on, turn-off angles by using various control strategies. Artificial neural networks and fuzzy-based methods mainly collect data and adapt the control parameters to real-time data, which allows the system to be more flexible [12].

1.1 Motivation and Objectives:

Switched reluctance motors attract considerable attention due to their simple and cost-effective construction, mechanical and thermal robustness, high power density, wide speed range and high reliability. Most of the conventional approaches have low efficiency but suffer from long training times, high computational costs and complex control design. Existing SRM control methods reduced torque ripple, but still suffer from limitations such as overshoot, increasing settling time, speed oscillations and reduced efficiency. These issues affect the smooth and stable operation of SRM drives. Therefore, this work motivated to develop an efficient torque ripple minimization approach using a cascaded fraction order controller integrated with hybrid optimization to improve speed regulation, reduce error and enhance overall SRM performance. The objective of the proposed approach is;

- ✓ To develop a TSF-based control strategy for effective torque ripple minimization in SRM drives.
- ✓ To design a novel cascaded fractional-order controller (FOPIT–FOPI–(1+PIDN)) for improved speed and current regulation.
- ✓ To propose a hybrid Salamander Orangutan Optimization Algorithm for simultaneous optimization of controller parameters and commutation angles.
- ✓ To minimize torque ripple and tracking error while ensuring smooth torque distribution among phases.
- ✓ To validate the effectiveness of the proposed control scheme using MATLAB/Simulink simulations.

The remainder of this research article is structured as follows: Section 2 discusses the most recent relevant works to SRM. Section 3 explains the proposed methodology with mathematical formulation, and Section 4 presents the evaluation results of the proposed framework. Finally, Section 5 concludes the entire research with future scope.

2. Literature Survey

Some of the recent existing works related to torque ripple, noise and optimization algorithms are listed as follows;

Oloo et al. [13] suggested a novel torque ripple minimization for SRM by an optimization algorithm. By selecting suitable turn-on and turn-off angles, the torque ripples in the SRM can be reduced. The model combines Harris hawks optimization (HHO) and radial basis function to search and estimate optimal switching angles. CCC implemented the method based on SRM 8/6, 600 V.

Karthikeyan et al. [14] introduced a novel enhanced adaptive sliding mode control (ASMC) with optimization for reducing the torque ripple in SRM. The design process begins with 8/6 SRM, and the effectiveness of the proposed ASMC reduces the ripple. The tuning of system parameters and the system performance was achieved by Termination parallelism Cooperative optimization (TPCO).

Deepak et al. [15] recommended a novel SRM drive using a modular multiport cascaded converter (MMCC) and an advanced direct torque control method. This system minimizes torque ripples and harmonic distortion while enhancing the SRM drive via the direct torque control strategy (DTC). The hardware performance enhanced the performance by validating the speed, torque and phase current measurement. This model achieved 41.5% reduced torque ripple and enhanced dynamic performance.

Jing et al. [16] proposed a novel reduced torque ripple for SRM by the neural network method. The electromagnetic torque ripple is analysed using an indirect torque control method. The current reshaping neural network (CRNN) is used to optimize current sharing and minimize torque ripple.The results for the method are implemented under various operating points.

Ismael et al. [17] suggested a novel torque sharing function (TSF) for SRM using an optimization algorithm. The TSF method improves the speed for varying conditions. The ant colony optimization (ACO) algorithm is designed to optimize the TSF and also tunes the parameter. The SRM suffers from torque ripple, speed oscillations and reduced efficiency, which leads to mechanical stress, vibration and noise.

Li et al. [18] developed a novel control strategy to lower the torque ripple and to improve the distribution rejection capability of the SRM. The system integrates model predictive control (MPC) with direct instantaneous torque control (DITC). The TSF method generates the reference torque profile. The results obtained from the simulation are a reduced steady-state torque ripple by 19.4% and shortens dynamic recovery time by 40%. Table 1 shows the summary of the existing work.

Table 1: Summary of Existing Work

Author's	**Method**	**Motor**	**Advantages**	**Disadvantages**
Oloo et al. [13]	HHO	8/6 SRM	Reduced torque ripple	Increased cost of construction
Karthikeyan et al. [14]	TPCO	8/6 SRM	This system effectively reduces the ripple	High execution time
Deepak et al. [15]	MMCC	8/6 SRM	Faster dynamic response and reduced torque ripple	Complex control design
Jing et al. [16]	CRNN	12/8 SRM	Distributed current is directly used in the SRM drive.	Neural networks make it less interpretable.
Ismael et al. [17]	ACO	8/6 SRM	Reduced mechanical stress, improved reliability	Used only for the automotive sector.
Li et al. [18]	MPC-DITC	8/6 SRM	Improved robust performances against external disturbances	Constructing the machine is often impractical.

2.1 Problem statement

Several studies have been developed on SRM and have offered several limitations. Although [13] suggested torque ripple minimization for SRM by the Harris hawks optimization algorithm, it still faces challenges such as increased cost of construction. Similarly, [14-15] developed an adaptive sliding mode controller optimized using the termination parallelism cooperative optimization algorithm to minimize torque ripple and error. However, this method suffers from limitations such as overshoot and increased settling time. The torque sharing function for the SRM was implemented using a current reshaping neural network model in [16], but speed oscillations and efficiency limitations still lead to mechanical stress, vibration and acoustic noise. Furthermore, the control strategy presented in [18] reduces torque ripple and enhances disturbance rejection capability; however, SRM facing limitation such as complex control design and low-speed operation. Therefore, an efficient and robust control approach is required to overcome these limitations and further improve the overall performance of SRM drives.

3. Proposed Methodology

To achieve smooth and efficient operation of the switched reluctance motor, the proposed research develops an integrated control and optimization framework for torque ripple reduction. Since SRM performance is affected by torque ripple caused by double-salient geometry and phase commutation, the study focuses on reducing this issue through an advanced control strategy. Figure 1 shows the structure of the proposed methodology.

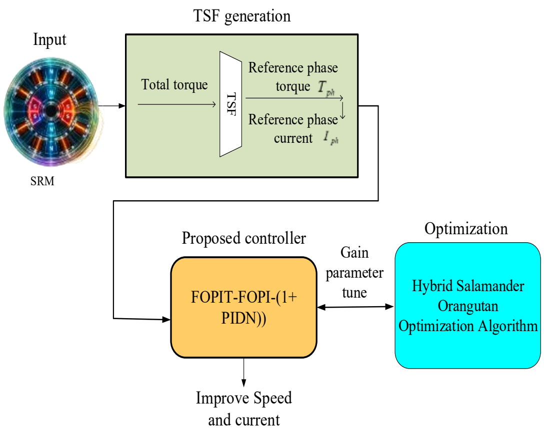

Figure 1: Overall workflow diagram

Initially, the 8/6 SRM model is developed, and its magnetic characteristics are analysis to current, speed, flux and torque generation. Then, the torque sharing function is applied to generate the reference phase torque. These TSF-based torque profiles are then converted into reference phase currents using flux and current characteristics. To regulate motor operation, a proposed cascaded FOPIT-FOPI-(1+PIDN)controller is designed for both speed control and current control. The controller parameters are optimized using a hybrid salamander-orangutan optimization algorithm. Finally, the proposed system is evaluated based on torque ripple reduction and tracking error minimization, resulting in smoother torque distribution, reduced vibration and enhanced overall SRM drive performance.

3.1 Modelling of Switched ReluctanceMotor

The 8/6 SRM motor control system regulates speed using a closed-loop mechanism with real-time feedback. Key parameters like speed and flux linkage are measured for performance evaluation. The distribution of eight stator poles and six rotor poles is symmetrical.The torque production in a switched reluctance motor is based on the minimum reluctance principle. Equation (1) for each phase in SRM can be described as follows,

$$V_{in} = I_s R_s + \frac{\beta(I,\alpha)\, d\lambda}{dt} \quad (1)$$

Here, $V_{in}, I_s R_s, \lambda$ represents the input voltage applied to each phase of the motor, current in the stator coil, and resistance of the stator and flux linkage and α is a rotor position. The mathematical model of SRM includes two fundamental equations, which are the equation of flux linkage and the equation for mechanical torque.

$$T_{ek} = \frac{d}{d\theta}\int_0^i \psi_k \, di_{ki} \quad (2)$$

$$T = T_e - T_L = J\frac{d\omega}{dt} + D\omega \quad (3)$$

Here, T_{ek} is the electromagnetic torque of phase winding, ψ_k is the flux linkage of phase winding, T_e and T_L represents the electromagnetic torque and load angular force, J is the moment of inertia and D is a fraction coefficient.

$$\psi_k = \psi(i_w,\theta) = L_a(\theta, i_w)\; i_k \quad (4)$$

where, i_w is the current phase winding and L_a represents the load angular force. So the torque expression is given as,

$$T_{ek} = -\frac{\partial W_k}{\partial \theta} \quad (5)$$

Here, ∂W_k is a winding electromagnetic energy and θ is rotor position angle. The following equation for torque generation T_g can be derived as,

$$T_g - T_l = B\omega + j\frac{d\omega}{dt} \quad (6)$$

where T_l B and j is the load torque, fraction coefficient and moment inertia, ω represents the rotor speed, respectively [19]. The 8/6 SRM mathematical model can be derived as follows:

$$\frac{di_l}{dt} = \frac{1}{i_l\frac{\partial l(\theta,i)}{\partial l} + L(\theta,i_{ph})}\left[N_r - \omega_j\right] \quad (7)$$

Here, N_r is the number of rotor poles, ω_r is the rotor speed calculated, i_l and is the current winding phase. The SRM modelling supports performance analysis, torque ripple reducing, speed regulation and controller design for achieving smooth and efficient motor operation.

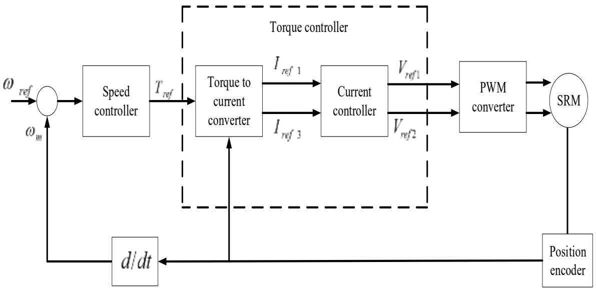

Figure 2: SRM drive system based on current control strategy

3.2 Torque Sharing Function for Switched Reluctance Motor

The torque sharing function is a control strategy used in a switched reluctance motor to achieve smooth torque generating during phase commutation. It distributes the required torque between the outgoing phases and incoming phases in a controlled manner, ensuring that the reduction in torque produced by the outgoing phase is compensated by the increase in torque generated by the incoming phase. By generating a smooth reference torque for each phase, TSF minimizes torque ripple and reduces vibration and noise to improve the overall performance of the SRM drive. First, the torque reference T_{ref} is obtained by processing the speed signal through an outer loop speed controller.

$$T_{ref} = \begin{cases} 0 & 0 \le \theta < \theta_{on} \\ T_n, f_{rise}\ (\theta) & 0_{on} \le \theta < \theta + \theta_{ov} \\ T_{ref} & 0_{on} + \theta_{ov} \le \theta < \theta_{off} \\ T_{ref}\ , f_{fall}(\theta) & 0_{off} \le \theta < \theta_{off} + \theta_{ov} \\ 0, & \theta_{off} + \theta_{ov} \le \theta < \theta_u \end{cases}$$

(8)

Here, $\theta_{on,}\, \theta_{off}$, $and\ \theta_{ov}$ represents the turn-on, tune-off, overlap angles, $T_n, f_{rise}\ and\ f_{fall}$ is the increasing position torque, required torque and decreasing portion torque, θ is the rotor position. The TSF incoming phase $f_{rise}\ and\ f_{fall}$ is present in equation (9-10),

$$f_{rise}\ (\theta) = 0.6 - 0.6\cos\left(\pi\frac{\theta - \theta_{on}}{\theta_{ov}}\right)$$

(9)

$$f_{fall}(\theta) = 0.6 + 0.6\ \cos\left(\pi\frac{\theta - \theta_{off}}{\theta_{ov}}\right)$$

(10)

Here, $f_{rise}\ and\ f_{fall}$ is the rising and falling position of TSF. The TSF generated the reference phase torque T_{ref} , which it converted into the corresponding reference phase current I_{ref} and flux f_j using the SRM torque-current position characteristics. The rotor position and current cause a nonlinear change in the SRM flux characteristic. Therefore, the reference torque is generated from the reference current,

$$I_{ref} = \frac{V_{dc} - \eta + P_j}{L(I,\theta)}$$

(11)

As can be observed, for a given current with constant V_{dc} and P_j , I_{ref} is the reference current. The stator flux linkage vector can be expressed as follows,

$$\psi_s = \int(\upsilon - I\vec{R} + S_c)\ dt$$

(12)

Here, ψ_s is the stator flux vector, υ is the stator voltage vector, IR is the stator current and stator resistance and S_c is the speed controller [20]. Thus, the torque sharing function ensures smooth torque transfer between SRM phases during commutation, maintaining nearly constant total torque and significantly reducing torque ripple, vibration and acoustic noise.

3.3 Proposed controller using Cascaded fractional order proportional integral tilt and fractional order proportional integral with one plus proportional integral derivative filter

In this section,a cascaded fractional-order proportional-integral tilt and fractional-order proportional-integral with one plus proportional integral derivative filter (FOPIT-FOPI-(1+PIDN)) controller is proposed. The proposed cascade controller is a two-stage control strategy developed to improve current regulation and speed control performance in the SRM drive system. The FOPIT controller is employed in the outer speed control loop, while the FOPI-(1+PIDN) controller is utilized in the inner current control loop. The cascaded structure enables accurate speed regulation and fast current tracking.Therefore, a hybrid controller can enhance system response by providing increased robustness, flexibility, and an improved ability to reject disturbances.

3.3.1 FOPIT

Fractional calculus is used by the FOPIT controller to further increase stability and boost system performance. The gains of the three terms in a PIT (proportional, integral and tilt) controller can be adjusted to manage transient response, rise time, overshoot, stability and steady-state errors. The structure of this controller can be rewritten as follows [21].

$$C_{FOPIT}(S) = \frac{Y(S)}{E(S)} = K_P + \frac{K_i}{S^{\lambda}} + K_t S^{(1/n)} \quad (13)$$

The FOPIT controller contains fivetunable parameters, namely proportional gain, K_p integralgain K_i ,tiltedgain K_t , fractional integral order λ and tilt exponent n .In additionally, including the fractional integrator minimizes the steady state error and provides higher flexibility due to the extra operator in the fractional part.

3.3.2 FOPI-(1+PIDN)

The FOPI controller provides and improves tracking accuracy and reduces steady-state error, and the PIDN controller improves response speed, enhances stability and reduces noise effects using the derivative filter. The FOPI-(1+PIDN) controller achieves faster response, lower tracking error, reduced oscillations, improved stability and smoother overall operation. The transfer functions of the FOPI-(1+PIDN) controller is expressed as follows;

$$C_{F0PI}(S) = \frac{Y(S)}{E(S)} = K_p + \frac{K_i}{S^{\lambda}}$$

(14)

here, $G_{FOPI}(S)$ is the transfer function of the FOPI controller, $K_p K_I$ is proportional and integral gain and S is the Laplace variable. The 1+PIDN is expressed as follows,

$$C(S)_{(1+PIDN)} = 1 + K_p + \frac{K_i}{S} + \frac{K_d N}{S+N}$$

(15)

Here, G_{PIDN} is the PID with derivative filter, K_D represents the derivative gain, N is derivative filter coefficient [22].The FOPI-(1+PIDN)combines a fractional order PI controller with a filtered PID controller to achieve faster response, lower steady-state error and better stability. The dynamic model for error to minimize is taken as,

$$e(t) = \omega_{ref} - \omega_{act} \quad (16)$$

Here, ω_{ref} represents the rotor speed in the reference model, ω_{act} and is the actual rotor speed. The FOPI-(1+PIDN) controller expressed as;

$$C(S)_{FOPI-(1+PIDN)} = \left(\left(K_P + \frac{K_i}{S^{\lambda}}\right)\left(1 + K_p + \frac{K_i}{S} + \frac{K_d N}{S+N}\right)\right)$$

(17)

The combined cascaded controller is mathematically expressed in the following equation,

$$C_{\text{Proposed}}(S) = C_{FOPIT}(S) \times C_{FOPI}(S) \times C_{(1+PIDN)}(S) \quad (18)$$

Figure 3: illustrates the block diagram of the FOPIT-FOPI-(1+PIDN) controller.

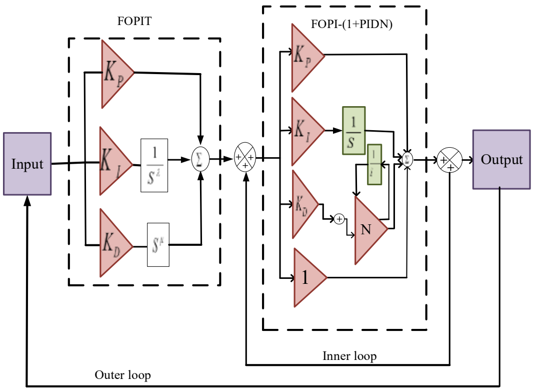

Figure 3:Block diagram of FOPIT-FOPI-(1+PIDN) controller

To achieve effective current and speed control in the SRM drive, the HSOA is employed to determine the optimal tuning parameters. The proposed FOPIT-FOPI-(1+PIDN) controller achieves fast dynamic response, reduced overshoot, and faster settling time.

3.4 Hybrid Salamander Orangutan Optimization Algorithm (HSOA)

The gain parameters of the controller are optimally tuned by HSOA. In the proposed work, the HSOA is utilized to optimize the controller parameter. The hybrid optimization algorithm is used to optimize parameters such as controller gains and commutation angles. The optimization process evaluated different parameter combinations that achieve minimum torque ripple, tracking error and improve speed. The salamander optimization algorithm performs global exploration, which helps search across a wide solution space and avoids getting trapped in local optimum solutions. The orangutan optimization algorithm performs local exploitation, which refines the selected solutions and improves convergence toward the optimal result. By combining these two optimization methods, the hybrid algorithm efficiently tunes controller parameters such as gain parameters and commutation angles. The position of each individual refers to: Each solution point $X_j : x_{j,i}$ is initialized at random within the constraints of the choice variables using equation (19).

$$X = \begin{bmatrix} X_{1,1} & \cdots & X_{1,1} & \cdots & X_{1,n} \\ \vdots & \ddots & \vdots & \iddots & \vdots \\ X_{j,1} & \cdots & X_{j,i} & \cdots & X_{j,n} \\ \vdots & \iddots & \vdots & \ddots & \vdots \\ X_{M,1} & \cdots & X_{M,i} & \cdots & X_{M,n} \end{bmatrix} \quad (19)$$

$$X_j : x_{j,i} = lb + Rand \times (ub - lb) \quad (20)$$

In the above equation, X is the population matrix, n is the number of decision variables, M is the population's number of individuals, X_j is its j^{th} dimension, $Rand$ is a random number in the interval [0,1], lb_i and ub_i are the lower and upper bounds. At the same time, within the context of the motor control system, response characteristics are considered equally important. Consequently, speed is established as a performance indicator, and the integral of the time-weighted absolute error (ITAE) of speed is utilized as the fitness function.

$$J_{ITAE} = \int_0^t t\,|e(t)| + T_r dt \quad (21)$$

Here, t is the simulation time, $e(t)$ represents the error value and T_r is torque ripple reduced. The fitness function is used to minimize the controller error. As given in (22), the commutation angles are turn-on and turn-off,

$$f_{fall}(\theta) = 1 - f_{rrise}(\theta + \theta_{on} + \theta_{off}) \quad (22)$$

Here, θ_{on} and θ_{off} represent the torque production. The main objective used in the developed salamander optimization algorithm isto maximize the average torque,

$$F_{obj} = \min\left(\frac{T_r}{T_{rb}} + \frac{T_{avb}}{T_{av}}\right) \quad (23)$$

Where, T_{av} and T_r is the average torque and torque ripple, respectively. Their base values are designed as T_{avb} and T_{rb} respectively.

3.4.1. Exploration phase

In the exploration phase, the algorithm, inspired by the regeneration of a salamander, looks for new controller parameter combinations to avoid local minima, thus improving torque sharing and reducing torque ripple. This phase serves to improve global searching capability and better tune the controller parameters.

$$x_{j,i}^{Q1} = x_{j,i} + \left(Rand + \frac{t-T}{t}\right) \times (X_{Best,i} - x_{j,i})$$
(24)

In the above equation, $x_{j,i}^{Q1}$ is the j^{th} individual's new position in the exploration phase, $X_{Best,i}$ is the i^{th} dimensions best known solution, $Rand$ is a random number between [0,1], t is the maximum iteration and X is a number that is chosen at random as either 1 or 2. The individual position is changed if the new position results in an improvement in the objective function value:

$$X_j = \begin{cases} X_j^{Q1} & S_j^{Q1} < S_j, \\ X_j & else \end{cases}$$
(25)

Here S_j is the objective function value of the current location and S_j^{Q1} is the objective function value of the new position.

3.4.2. Exploitation phase

Taking inspiration from the orangutan ideal movement techniques, the algorithm fine-tunes the solution in the second phase by marginally changing individual placements to capitalize on possible areas discovered in the exploration phase. This phase optimizes the gain parameter tuned by the controller to minimize torque, reduce tracking error improved overall speed and current regulation.

$$x_{j,i}^{Q2} = x_{j,i} + \left(Rand + \frac{ub - lb}{t}\right)$$
(26)

In the above equation, $x_{j,i}^{Q2}$ is the j^{th} individual new position in the exploitation phase, $rand$ is random number in [0, 1]. The position is updated if the objective function improves:

$$X_j = \begin{cases} X_j^{Q2} & O_j^{Q1} < O_j, \\ X_j & else \end{cases}$$
(27)

Here O_j is the objective function value of the current location and X_j^{Q1} is the objective function value of the new position.

Algorithm 1 represents the pseudocode of HSOA.

Algorithm 1: Pseudocode of HSOA

Input: Gain parameter, commutation angles and objective function

Output: Best tunecontroller parameters

Step 1: Initialize population randomly within the lower and upper bounds

Step 2: Evaluate fitness F_{obj} for average torque

Step 3: Perform the salamanderorangutanoperation

Step 4: Define initial best solution

Step 5: For $t = 1$ to T do

Step 6: For each parameters X do

Step 7: Update

Step 8: Perform exploration updateusing global search

Step 9: Perform exploitation update using local search

Step 10: End For

Step 11: Retune

By integration exploration and exploitation, the proposed hybrid algorithm maintains a balance between global and local refinement. The optimization process determines the optimal controller gains and commutation angles that improve torque sharing, reduce torque ripple [23-24], enhance dynamic performance and smooth SRM operation. As a result, the proposed method minimizes torque ripple, reduces tracking error, improves speed regulation and enhances the overall performance and stability of the SRM system.

4. Result and discussion

To evaluate the performance of the proposed controller strategies, simulation results have been carried out using MATLAB/Simulink software. This section represents the simulation results for the proposed model. The simulation parameters are displayed in Table 2.

Table 2: Simulation parameters

Devices	Parameters	Values
	Type	8/6
	Stator resistance	0.065 Ω
	Inertia	0.02 kg.m.m
	Friction	0.02 N m/s
	Initial speed	0 rad/s
	Initial position	0 rad
	Sample time	2×10^{-5}
SRM	Unaligned inductance	0.00067H
	Aligned inductance	0.0236H
	Saturated aligned inductance	0.00015H
	Maximum current	250A

4.1 Constant input condition

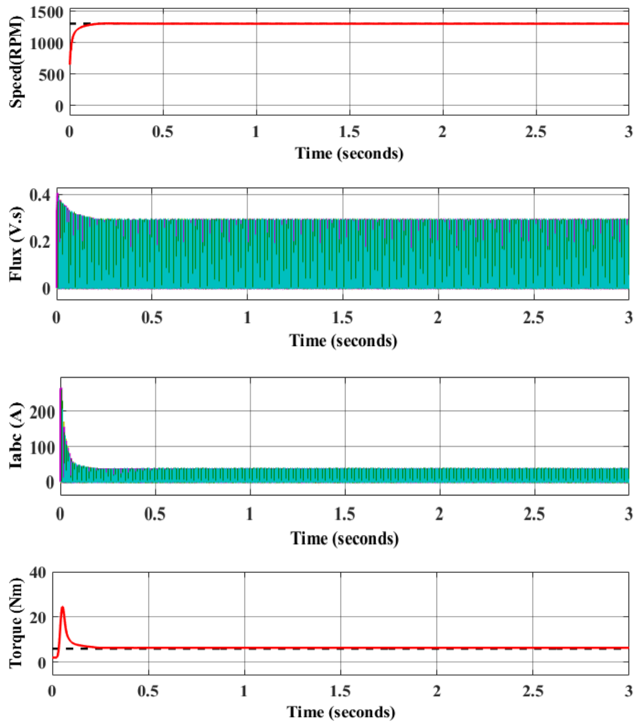

Figure 4: Simulation result for constant input operating condition

Figure 4 shows the dynamic performance of the motor system in speed, flux, current and torque with respect to time. The motor speed increases rapidly and reaches a stable value of approximately 1300 RPM, indicating fast response and effective speed regulation. The flux indicates a constant value of around 0.3 V.s, showing stable magnetic operation. Similarly, the phase current and torque is initial peak and then stabilize at a lower constant value, demonstrating a smooth torque response and reduced current fluctuations.

4.2 Varying input condition

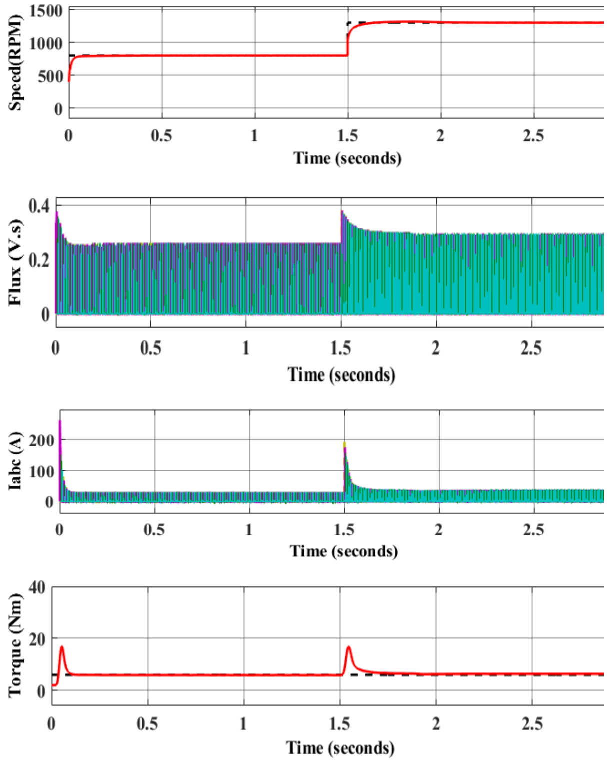

Figure 5: Simulation result for varying operating conditions

Figure 5 shows the dynamic performance of the motor system under a step change in operating condition at approximately 1.5 seconds. The motor speed increases rapidly and reaches a stable value of 800 RPM, demonstrating good tracking capability and fast response. The flux is initially small and transient and stabilizes around 0.3 V.s, which indicates stable flux control. The phase current shows a high starting current and then lowers to a lower constant value. The simulation results demonstrate fast dynamic response, stable speed and smooth torque performance under varying operating conditions.

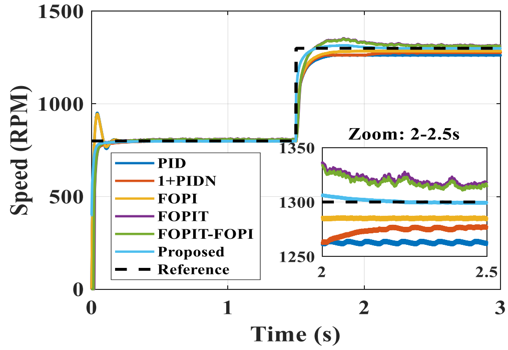

Figure 6:Speed performance analysis of different controllers

Figure 6 compares the speed analysis of the existing controllers with the proposed controller. The existing optimization algorithms, such as proportional integral derivative (PID), one plus proportional integral derivative filter (1+PIDN), fractional order proportional integral (FOPI), fractional order proportional integral tilt (FOPIT), fractional order proportional integral tilt - fractional order proportional integral (FOPIT_FOPI),are compared with the proposed algorithm. The speed performance at 1300 RPM shows the proposed method's stable operation and improved speed. The proposed controller reaches the reference speed faster with lower overshoots and reduced oscillations compared to the other controllers.

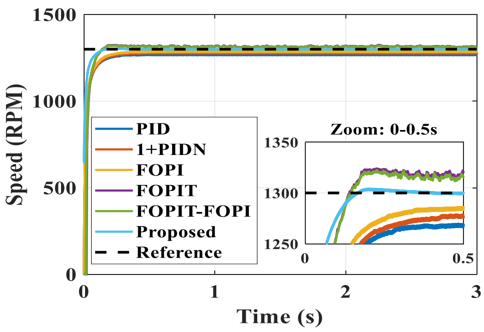

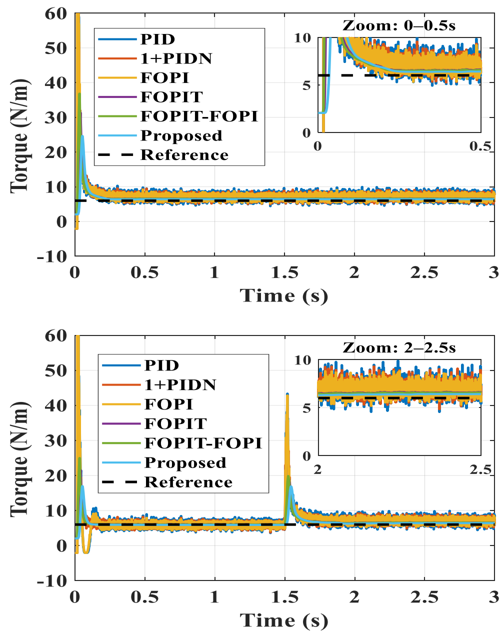

Figure 7: Torque performance analysis of different controllers

Figure 7 compares the torque analysis of the existing controllers with the proposed controller. Torque analysis evaluates several existing control mechanisms, including PID, 1+PIDN, FOPI, FOPIT, FOPIT and FOPIT-FOPI. The proposed controller exhibits improved torque tracking, reduced torque ripple and better dynamic performance than the conventional controllers. Figure 8 is an efficiency analysis with existing controllers.

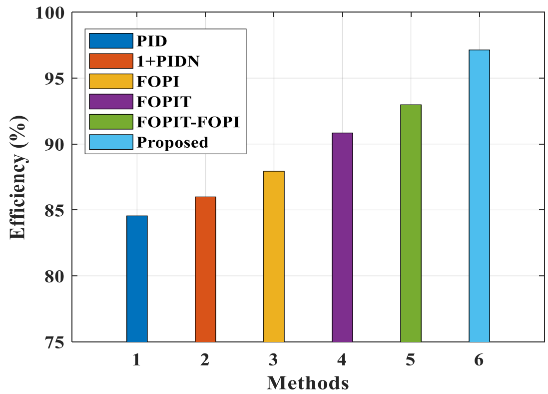

Figure 8: Analysis of Efficiency with Existing Controllers

Figure 8 illustrates the analysis of efficiency. The existing controllers have low efficiency compared to the proposed controller. The PID controller with 84.55% of efficiency, 1+PIDN contains 85.99%, FOPI controller is 87.94%, FOPIT controller contains 90.84%, and FOPIT-FOPI controller with 92.98%. The proposed model contains 97.14% efficiency. Thus, the controller is compared with other controllers that provide effective performance of the system. Then, an analysis of standard deviation (STD) is presented in Figure 9.

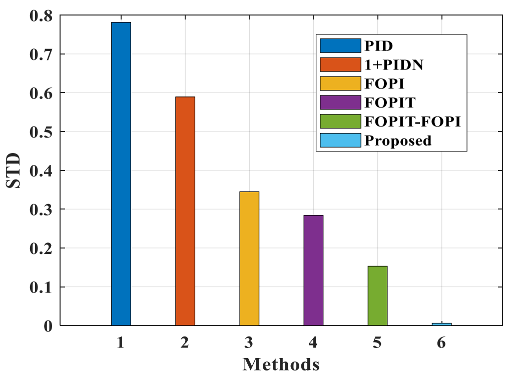

Figure 9:Analysis of standard deviation

Figure 9 illustrates the standard deviation (Nm) across different controller strategies. The existing controller achieves a higher value than the proposed controller. The previous PID and 1+PIDN yield STD values of 0.781% and 0.589, which are higher than the suggested model. The FOPI and FOPIT obtained STD values of 0.452% and 0.284%, and the FOPIT-FOPI controller contains 0.153%. Furthermore, the proposed controller obtained a lower STD value of 0.006%. Then, an analysis of the ripple is presented in Figure 10.

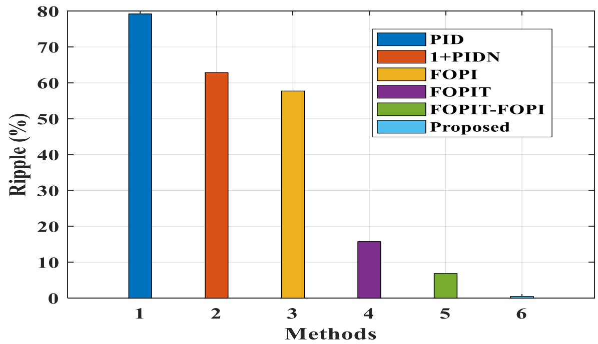

Figure 10: Analysis ofRipple

Figure 10 illustrates the analysis of ripple. The controllers compared: PID, 1+PIDN, FOPI, FOPIT, FOPIT and FOPIT-FOPI. The ripple obtained by the PID controller was 79.2%, the 1+PIDN controllers at 62.84%, the FOPI controller at 57.72%, the FOPIT controller at 15.74%, and the FOPIT-FOPI controller at 6.84%. Compared to other controllers, the proposed controller achieve lower ripple of 0.45%. The proposed technique maintains the stability compared to other conventional methods.

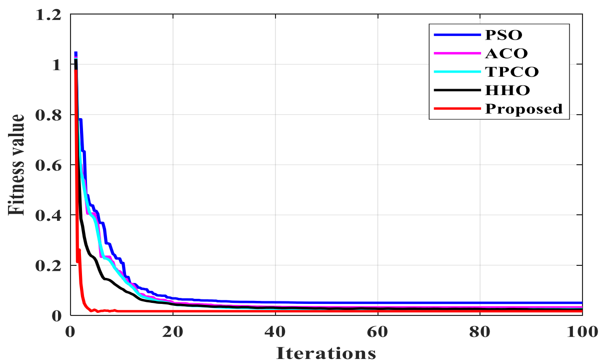

Figure 11: Analysis of Fitness values

Figure 11 depicts the convergence plot of the proposed method. Here, PSO represents particle swarm optimization, ACO denotes ant colony optimization, TPCO represents topology optimization, and HHOA denotes the Harris hawks optimization algorithm. The proposed algorithm is compared with the PSO, ACO, TPCO and HHOA, which results in reduced fitness values. The proposed method achieves the lowest final fitness, which is the best solution compared to other algorithms.

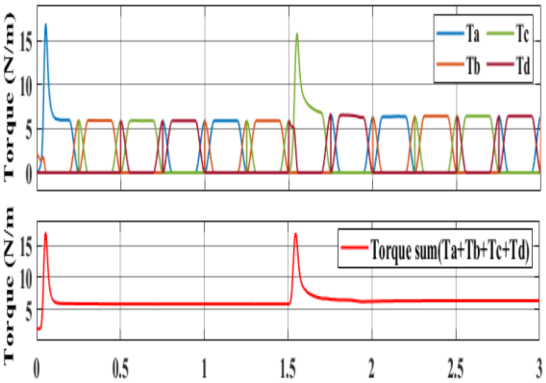

Figure 12: Torque profiles of four actuators and combined torque output

Figure 12 shown the torque produced by four phases Ta, Tb, Tc, and Td and total torque are combining of allphases. The Ta, Tb, Tc, and Td analysis is represented the torque produced by each phase. The total torque is (Ta + Tb + Tc+ Td) is individual phases torque, in this torque is constant at 6 N.m for most of the operations. In this analysis torque effectively shared among the four phases ensure a stable and smooth total torque output.

Table 3 shows the performance evaluation of different controllers. These controllers are implemented in a Simulink model, and the results are obtained for evaluation. The efficiency for the proposed model is 97.14%; it is high when compared to existing work. Comparing all this performance with the different controllers, the proposed methods have high efficiency and low ripple and settling time.

Table 3: Performance evaluation of different controllers

Controller	**Max Torque (Nm)**	**Min Torque (Nm)**	**Efficiency (%)**	**Std Deviation (Nm)**	**Ripple (%)**	**Ripple Coefficient**	**Settling Time (s)**
PID	9.9745	4.38	84.55	0.7813	79.2	0.1106	0.1125
1+PIDN	9.3845	4.826	85.99	0.5892	62.84	0.08654	0.1324
FOPI	9.0892	5.0876	87.94	0.5522	57.72	0.0797	0.1443
FOPIT	8.6821	5.3684	90.841	0.284	15.74	0.05841	0.1014
FOPIT+FOPI	7.1658	5.8462	92.98	0.153	6.84	0.01024	0.0985
Proposed	**6.8205**	**6.8032**	**97.14**	**0.006**	**0.45**	**0.0009**	**0.0364**

5. Conclusion

This work presents an effective control and optimization approach for reducing torque ripple in the SRM drive system. The proposed method combines TSF with a hybrid salamander-orangutan optimization algorithm to achieve smooth torque distribution and improve motor performance. The SRM modelling is developed, and its magnetic characteristics are analysed to generate accurate reference phase torque profiles. These torque profiles are then converted into reference current based on flux and current characteristics. To improve control performance, an FOPOT-FOPI-(1+PIDN) is introduced for speed and current regulation. The controller parameters, together with commutation angles, are optimally tuned using the proposed hybrid optimization algorithm. The outcomes and implementation of the proposed method for torque ripple minimization in switched reluctance motor drives are done using the MATLAB/Simulink tools. Existing controllers such as PID, 1+PIDN, FOPI, FOPIT, FOPIT and FOPIT-FOPI contain less efficiency and high computation complexity compared to the proposed controller. The proposed method has a high efficiency of 97.14%,an average torque of 6.8205 Nm and achieves the average output power of 3346.07 W. The salamander orangutan optimization algorithm is used to fine-tune the gain parameter and commutation angle. Future work will focus on investigating the applicability of the proposed controller in an electric vehicle drive and high-performance industrial motor application to improve overall reliability and operational efficiency.

Reference:

1. Mohanraj, Deepak, DevakirubakaranSamithas, Praveen Kumar Balachandran, and Muhammad AmmirrulAtiqiMohdZainuri. "An Improved Power Factor Correction Converter for Switched Reluctance Motor Drive Performance Analysis." IEEE Access (2025).
2. Kachapornkul, Seubsuang, RuchaoPupadubsin, PakasitSomsiri, PraponJitkreeyarn, and KanokvateTungpimolrut. "Performance improvement of a switched reluctance motor and drive system designed for an electric motorcycle." Energies 15, no. 3 (2022): 694.
3. Sreeram, K., P. K. Preetha, Rodríguez-García Javier, and Álvarez-Bel Carlos. "A comprehensive review of torque and speed control strategies for switched reluctance motor drives." CES Transactions on Electrical Machines and Systems 9, no. 1 (2025): 46-75.
4. Cai, Jun, Xiaolan Dou, Adrian David Cheok, Ying Yan, and Xin Zhang. "Overview of the direct torque control strategy in switched reluctance motor drives." IEEE Transactions on Transportation Electrification 11, no. 1 (2024): 1617-1628.
5. Diao, Kaikai, Xiaodong Sun, Gang Lei, YouguangGuo, and Jianguo Zhu. "Multiobjective system level optimization method for switched reluctance motor drive systems using finite-element model." IEEE Transactions on Industrial Electronics 67, no. 12 (2020): 10055-10064.
6. Lan, Yuanfeng, YassineBenomar, Kritika Deepak, AhmetAksoz, Mohamed El Baghdadi, EmineBostanci, and Omar Hegazy. "Switched reluctance motors and drive systems for electric vehicle powertrains: State of the art analysis and future trends." Energies 14, no. 8 (2021): 2079.
7. Al-Amyal, Fahad, LászlóSzámel, and Mahmoud Hamouda. "An enhanced direct instantaneous torque control of switched reluctance motor drives using ant colony optimization." Ain Shams Engineering Journal 14, no. 5 (2023): 101967.
8. Ibrahim, Muhammed A., and Ahmed Nasser B. Alsammak. "Dynamic modelling and current control for switched reluctance motor drives in electric vehicles." In IOP Conference Series: Materials Science and Engineering, vol. 1295, no. 1, p. 012006. IOP Publishing, 2023.
9. Wang, Xudong, YasamanNiazi, SadraTavakolian, AzadehGholaminejad, Gaoliang Fang, SumedhDhale, Diego F. Valencia, BabakNahid-Mobarakeh, and Ali Emadi. "A Review of Current Control Strategies for Switched Reluctance Motor Drives: Performance Evaluation Across a Wide Speed Range." IEEE Open Journal of the Industrial Electronics Society 7 (2025): 136-156.
10. Saleh, Ameer L., LászlóSzámel, Mohammad A. Abido, and Mahmoud Hamouda. "A Novel Reduced-Ripple Torque Control Technique for Electric Vehicle Switched Reluctance Motors Using an Adaptive Fuzzy Neural Network." IEEE Open Journal of Power Electronics 7 (2026): 1133-1150.
11. Saleh, Ameer L., Mahmoud Hamouda, LászlóSzámel, and Mohammad A. Abido. "Wavelet neural network-based reduced-ripple DITC of switched reluctance motors in electric vehicles." Scientific Reports (2026).
12. El-Hameed, Mohamed A., Mahfouz Saeed, Adnan Kabbani, and EnasAbd El-Hay. "Enhancing Performance of PEM Fuel Cell Powering SRM System Using Metaheuristic Optimization." Energies 18, no. 8 (2025): 2004.
13. Oloo, Jackson, and Szamel Laszlo. "Torque ripple minimization for switched reluctance motor drives based on Harris hawks–radial basis function approximation." Energies 18, no. 4 (2025): 1006.
14. Karthikeyan, G., and T. Suresh Padmanabhan. "Enhanced adaptive sliding mode control with

termination parallelism cooperative optimization for torque ripple reduction in switched reluctance motor drives." Scientific Reports 15, no. 1 (2025): 16174.

15. Deepak, M., K. Santhakumar, K. Sathiyasekar, BharatirajaChokkalingam, and SanjeevikumarPadmanaban. "Performance-driven switched reluctance motor drive using multiport cascaded converter and advanced direct torque control scheme." Scientific Reports 16, no. 1 (2026): 12211.
16. Jing, Benqin, Guofu Liang, Xuanju Dang, and Yanjun Jiang. "Reducing torque ripple for switched reluctance motors by current reshaping neural network." Scientific Reports 15, no. 1 (2025): 17530.
17. Ismael, Dhiyaa Mohammed, and Thamir Hassan Atyia. "Torque sharing function optimization for switched reluctance motor control using ant colony optimization algorithm." Int J POW Elec&DriSyst 16, no. 3 (2025): 1537-1551.
18. Li, Liuxi, Jingbo Wu, Yafeng Yang, ZhijunGuo, Hongyao Wang, and Shaofeng Li. "Cooperative MPC-DITC Strategy for Torque Ripple Suppression in Switched Reluctance Motors." World Electric Vehicle Journal 17, no. 3 (2026): 154.
19. Nagesh, K., D. Lenine, and P. Sujatha. "Modelling and analysis of 8/6 switched reluctance motor with PI controller." *Journal of Mechanics of Continua and Mathematical Sciences* 5 (2020): 357-370.
20. Al Quraan, Laith, Ameer L. Saleh, and Laszlo Szamel. "Indirect instantaneous torque control for switched reluctance motor based on improved torque sharing function." IEEE Access 12 (2024): 11810-11821.
21. Mohamed, Emad A., Ahmed Shawky, Sulaiman Z. Almutairi, MokhtarAly, Emad M. Ahmed, TarekKandil, and M. S. Hassan. "Optimal 1+ PDDF/FOPIT frequency regulator for developing robust multi-microgrid systems by employing EV energy storage batteries." Journal of Energy Storage 73 (2023): 109088.
22. Jabari, Mostafa, SerdarEkinci, DavutIzci, Mohit Bajaj, Vojtech Blazek, and Lukas Prokop. "A robust multi-stage FOPI (1+ PIDn) controller for precision control of switched reluctance motors under nonlinear and uncertain conditions." Energy Reports 15 (2026): 109231.
23. Hamadneh, Tareq, BelalBatiha, Oqlah Al-Refai, IbraheemKasimIbraheem, AseelSmerat, Frank Werner, ZeinabMontazeri et al. "Salamander optimization algorithm: a new bio-inspired approach for solving optimization problems." Int. J. Intell. Eng. Syst. 18, no. 7 (2025): 550-561.
24. Hamadneh, Tareq, BelalBatiha, GharibMousaGharib, ZeinabMontazeri, Frank Werner, GauravDhiman, Mohammad Dehghani et al. "Orangutan optimization algorithm: An innovative bio-inspired metaheuristic approach for solving engineering optimization problems." Int. J. Intell. Eng. Syst 18, no. 1 (2025): 45-58.